

We are IntechOpen, the world's leading publisher of Open Access books Built by scientists, for scientists

6,900

Open access books available

186,000

International authors and editors

200M

Downloads

Our authors are among the

154

Countries delivered to

TOP 1%

most cited scientists

12.2%

Contributors from top 500 universities



WEB OF SCIENCE™

Selection of our books indexed in the Book Citation Index
in Web of Science™ Core Collection (BKCI)

Interested in publishing with us?
Contact book.department@intechopen.com

Numbers displayed above are based on latest data collected.
For more information visit www.intechopen.com



A Structural Health Monitoring of a Pitch Catch Active Sensing of PZT Sensors on CFRP Panels: A Preliminary Approach

K.D. Mohd Aris, F. Mustapha, S.M. Sapuan and D.L. Majid

Additional information is available at the end of the chapter

<http://dx.doi.org/10.5772/48097>

1. Introduction

At present, the advanced composite materials have gained its acceptance in the aerospace industries. The content of these materials has increased dramatically from less than 5% in the late eighties to more than 50% at the beginning of this decade. [1] The materials offer high strength to weight ratio, high strength to weight ratio, corrosion resistance, high fatigue resistance etc. These benefits have transformed the aviation world traveling to better fuel consumption, endurance and more passengers. However, the use of these materials has posed new challenges such as impact, delamination, barely visible internal damage (BVID) etc. Before a part or component being used on the actual structure, they are being tested from small scale to the actual scale in a controlled environment either at lab or test cell. However the attributes imposed during the operation sometimes shows different behavior when the actual operations are performed due to environment factors, human factors and support availability. To ensure the safety is at the optimum level, the continuous conditional monitoring need to be carried out in order to ensure the component operate within the safety margin being placed by the aircraft manufacturers. [2] One of the areas under investigation is the structural integrity assessment through the use of non-destructive inspections (NDI). The NDI allows aircraft operator to seek information on the aircraft structure reliability by inspecting the structure without having to remove it. There are many types of inspection methods which are limited to materials, locations and accuracy depends on methodology applied. [3] Few of popular techniques are eddy current, ultrasonic, radiography, dye penetrant which have been existence in quite a time. However due to composite material applications new methods have emerged in order to improve detection to attain converging results such as tap test, laser shearography, phase array etc.. So far, these methods prove its effectiveness and consistency in finding the anomalies.

However these techniques require total grounding of the aircraft and the inspection are manually intensified. The only clue where to inspect the area from the occurrence report, maintenance schedule or mandatory compliance by the authority. New inspection paradigm need to be developed as defects will arise in the non-conventional ways as the composite materials being used in the pressurized area such as in Boeing 787 and Airbus A350 aircrafts. Therefore, the available methods need to be systematically chosen depends on thin laminate, thick laminate or sandwich structure.[4] The active monitoring offers continuous monitoring either by interrogating or listen to the structure behavior. Embedded sensor and on surface sensors offers the advantages and disadvantages that yet not being explored fully and can accommodate the NDI techniques. The structure integrity will behave differently as the structure being modified and repair to ensure continuation of the aircraft operation and prolong its service life. The aircraft structural health monitoring (SHM) is one of the conditioning monitoring that has gained its usefulness. Such health monitoring of a component has been successfully being used in the aircraft avionics systems, engine management systems, rotary blade systems etc. Since the SHM is still at its infant stage, several methodology and detection methods are been explored to suite the monitoring purposes. Acoustic emission, fiber bragg grating, compact vacuum monitoring etc. are being investigated for their potential. [5] Therefore the paper is focusing on issues on the implementation of the SHM at post repair through the use of PZT sensor by using guided waves as a method of monitoring for active and passive structural surface conditions.

2. Theoretical background

The use of advanced composite materials has shifted the paradigm in aircraft structure design, operation and maintenance philosophy. A simple stop drills procedure is used to prevent further propagation of crack or by removing the damage area and replacing the damage area. This procedure are well written in typical aircraft structural repair manual (SRM) under Chapter 50-xx-xx found in the ATA 100 (Air Transport Associations) [6]. The procedure above can only be applied to metallic structure since the behavior is isotropic in which properties such as damage tolerance, fracture mechanics and fatigue can be predicted although the repair has been done on the damaged structure. The composite structures are made up from various constituents that are laid up and bonded together with the assistance of pressure and temperature at predetermine times. During operations, the aircraft structures are subjected to damages due to impact, environmental, residual imperfections, delaminations that reduces the structural integrity of the aircraft [7]. Typically, there are four types of repair applied to the composite structures. There are external bonded patches, flush or scarf bonded repair, bolted patch and bonded patches [8]. This operation requires the strength to be returned back to the original strength [9]. Due to the orientation, number of plies and materials used the level of recovery of the operating strain is much dependent on the stiffness of the laminates. The governing equation for the actual load to be transmitted to the new repaired laminates are given by the equation below [10] & [11]

$$P=e_a E_x t \quad (1)$$

Where, P , ϵ_a , E_x , and t are actual load, ultimate design strain, modulus in the primary loading direction and the laminate thickness respectively. A simple calculation of the strength of materials can be applied to scrutinized the scarf joint for the maximum allowable stress [10] & [11]. The equation is given by

$$P_{\max} = \sigma_u t \leq \frac{\tau_p t}{\sin \theta \cos \theta} \quad (2)$$

Where P_{\max} , σ_u , t , θ and τ_p is the maximum load, ultimate stress, thickness, shear stress and scarf angle respectively. By solving the value of θ , the scarf angle is found to be at 2° or at 1:30 ratio in order to attained minimum ultimate stress for the repair structure strength to be similar with the parent structure.

Studies have shown the use of PZT sensors on experimental aircraft component such as flaps and wings are promising [12] and [13]. For this experiment, an aircraft spoiler was used as the experimental subject by mounting the sensor arbitrarily on the spoiler's surface. The sensor can also be used to detect the surface condition of normal, damaged and repaired structures.

Most of the structural damage diagnoses were predicted by using analytical or finite element modeling [14], [15] and [16]. Although the results were accepted but it requires a powerful computing hardware, labor intensive interaction and modeling errors before a solution can be converged. Another method is to utilize the statistic to evaluate the captured data. However large amount of data are required to achieve higher reliability and probability to converge to the intended solution. The statistical approach utilizes supervised and unsupervised learning in order to process the data. [17] and [18] The supervised learning uses data as its references and the unsupervised learning uses to cluster the data and group them for selective conditions. The approach can be achieved by using the Statistical Pattern Recognition [19]. The principles in SPR are:-

1. Operational Evaluation,
2. Data Acquisition & Cleansing,
3. Feature Extraction & Data Reduction and
4. Statistical Model Development or Prognosis

Only no 1 and 2 were concerned in this paper.

Outlier Analysis is one of the method applied in SPR. The OA is used as the detection of cluster, which deviates from other normal trend cluster. One of the most common discordance tests is based on the deviation statistic [19] given by

$$z_i = \frac{d_i - \bar{d}}{\sigma} \quad (3)$$

where z_i is the outlier index for univariate data, d_i is the potential outlier and \bar{d} and σ are the mean sample and standard deviation. The multivariate discordance test was known as Mahalanobis square distance given by

$$Z_i = (\{x_i\} - \{\bar{x}\})^T [S]^{-1} (\{x_i\} - \{\bar{x}\}) \quad (4)$$

where Z_i is the outlier index for multivariate data, x_i is the potential outlier vector and \bar{x} is the sample mean vector and S is the sample co-variance matrix [20] and [21]. The result of the above equation is congregated when the distance of a data vector is higher than a preset threshold level.

3. Experimental setup

There were two experimental procedures were taken place. The first was the study of the wavelet through an aircraft part at normal, damaged and repaired conditions. The second is to observed the guided Lamb wave behavior when subjected to tensile loading for the three conditions stated above.

The APC 850 PZT sensor from APC International Inc. was used for both experiments. The properties of the sensors are shown in Table 1 below. Two sensors were used as an actuator and receiver with a diameter of 10mm and thickness of 0.5mm. The pitch catch active sensing was used to obtain the data at the receiving sensors. The sensors were placed at 100mm apart due to the optimum wave attenuation from the actuator to the receiver. The actuator was connected to a function generator where a selected input variable were set and the receiver were connected to the oscilloscope for data mining and further processing.

Description	Value
Voltage limit AC/DC	8/ 15 V
Output Power	20 watts/ inch
Relative dielectric constant	1750
Dielectric loss	1.4%
Curie Temperature	360°C
Density	$7.7 \times 10^3 \text{ kg/m}^3$
Young's Modulus	$6.3 \times 10^{10} \text{ N/m}^2$

Table 1. APC-850 properties [22]

3.1. Aircraft component analysis

An aircraft spoiler was used for this research. The use of the structure is only arbitrary at this stage. It is use to seek the workability of the sensor upon trial on several flat panels. Three conditions were introduced to the panel which is the undamaged/ parent, damaged and repaired area. The undamaged/ parent was the area free from any defects. The undamaged area is the original conditions or controlled area. The damaged area was damage caused by impact that removes the top laminate. It was made by impacting the faced planes with a blunt object and creating damage less than 40mm diameter fracture. The level of impact is not an interest in this particular testing due to the studied conditions is only applicable to small surface damage due to impact. The repaired area was where the

damage plies were removed and replaced in accordance with the SRM [23]. The damaged area was repaired by scarfing method.



Figure 1. Locations of the structural conditions and PZT sensor placements

The repair was conducted by using hot bonder from Heatcon Inc. The Hexply® M10/38%/UD300/CHS/460mm CFRP pre-preg system from Hexcel Corp was used for the repair process. Care and take were observed to ensure similar procedures as per SRM recommendation. All plies were cut according to the sizes required and laid up accordingly. The affected area were vacuum bag as per Figure 2 and cured at 120°C at atmospheric pressure for 120 minutes. All vacuum bag materials were removed once the cycle ended.

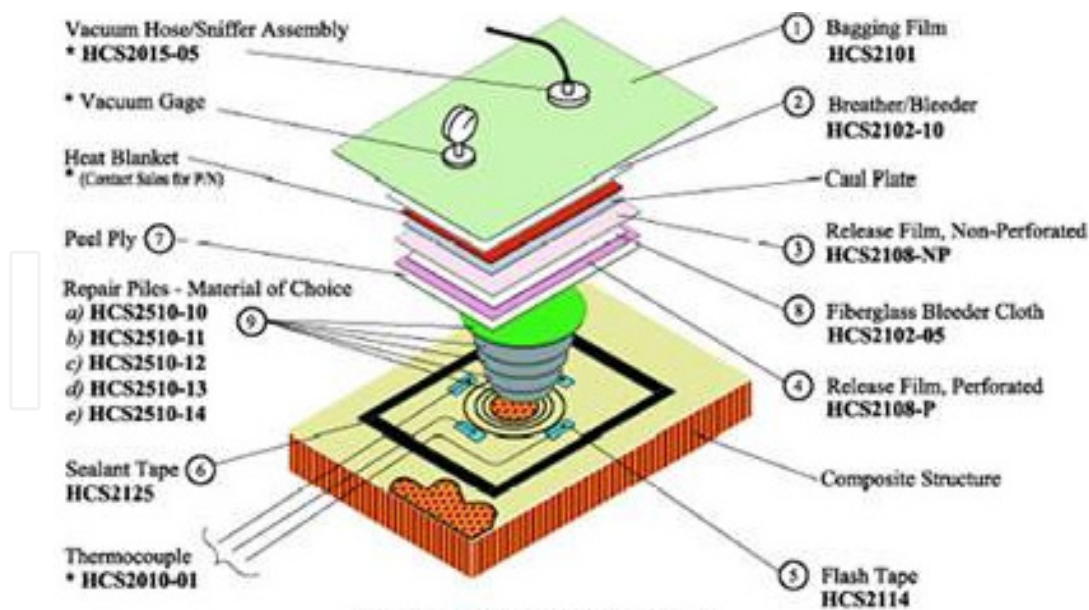


Figure 2. Hot bonder materials sequence for repairing aircraft composite parts. [24]

The PZT sensors were placed at 100mm apart for the three studied conditions. For damaged condition, the sensors were placed in between the damage area and for the repaired area, the sensors were replace across the actual and the repair doubler surface. This is to ensure

distance consistency of 100mm between the sensors. One of the sensors acted as an actuator. The actuator controls the surface guided in the form of elastic perturbation through the surface guided wave across the panel. The wave was controlled by a function generator with the setup as per Table 2.

Parameter	Unit	Parameter	Unit
Frequency	250kHz	Symmetrical	50%
Voltage	+10V	Time Generation	3ms at 333.3 Hz
V_{pp}	50Ω	Burst Count	5
Phase	0°		

Table 2. Actuating setting parameter.

The receiving sensor modulated as the guided wave reached and transmit the energy to electrical signal. The received signals were saved for post processing by using oscilloscope. The arrangement of the equipment is shown in Figure 4.

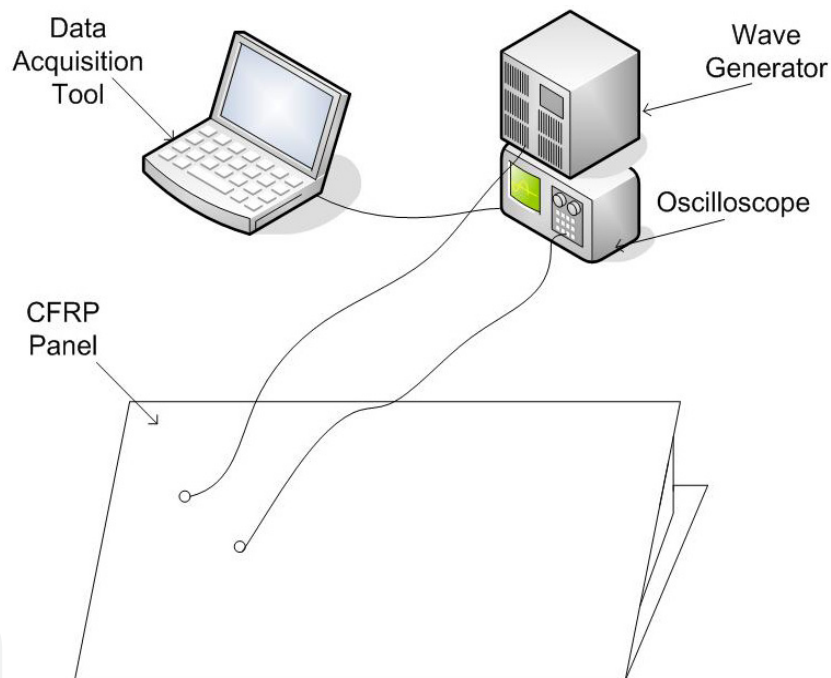


Figure 3. Aircraft spoiler with PZT sensor on specimens set-up.

3.2. Tensile testing

Further investigation was conducted by using 2 sets of tensile testing specimens with condition of normal and repair attached with pair of PZT sensors. Three composite plate of 300mm by 300mm were fabricated by using the Hexply® M10/38%/UD300/CHS/460mm from Hexcel Corps. The ply orientation was set to $[0/90]_{s2}$ orientation to produce a balanced symmetrical flat monolithic structure. The parent specimen was subjected to one time curing. However the repaired specimens undergone for secondary curing once the damage area was removed and new replacement plies were laid up. Both initial and secondary

bonding was cured in accordance with Aircraft Structural Repair Manual (SRM). A scarf cutting technique was used to remove the damage and replaced the affected its areas. Curing was achieved by using the Heatcon HCS4000 hot bonder with assisted consolidation from vacuum bag as per Figure 2. The parameters were ramp rate at $3^{\circ}\text{C}/\text{min}$, dwell time at 120 minutes, dwell temperature at 121°C , cooling rate at $3^{\circ}\text{C}/\text{min}$ and vacuum pressure attained at 22 in mg/ 1 bar.

Once cured, the panels were cut into specimen size according to ASTM D638 standard with five specimens prepared for each conditions by using Shimadzu AGx-50kN Universal Testing Machine as per Figure 5. The specimens were clamped on both ends. The data for mechanical properties were collected by using the Trapezium-X software came with the UTM machine. For the wavelet pitch-catch analysis, two APC 850 PZT smart sensors were affixed at 100mm apart and symmetrical to each other. Similar connection with the spoiler's test was applied to the relevant apparatus for data mining and post processing. The data from the sensor was interrogated and collected at three stages which were at the beginning of the test, within the elastic range, after the detection of the first ply failure and prior to separation.

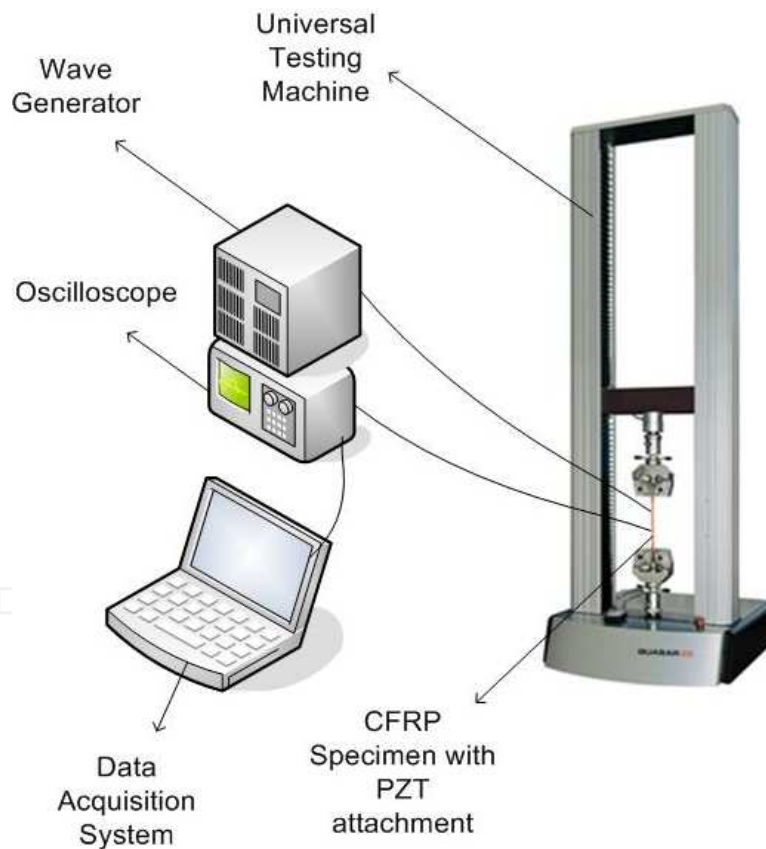


Figure 4. Tensile test with PZT sensor on specimens set-up.

4. Results and discussion

The results for both experiments are being presented into two sections. The initial test was evaluated upon the V_{pp} from the wavelet analysis. Further overlaying pattern are also

being presented. The latter testing involved with the tensile testing and only the results from wavelet analysis are shown accordingly.

4.1. Aircraft component analysis

Statistical pattern recognition was used to analyze the lamb wave generated by the PZT actuator. [15] A total of 100 wave packets were taken for each conditions stated. Each wave packets consisted of 25000 points by default from the oscilloscope. From the 25000 points, it was then grouped to 1000 intervals data set for analysis. There were two significant spike occurred each at point 12000 ~ 13000 and 18000 ~19000 as shown in Figure 4. The reduction of data intervals were applied in order to assist the further analyze the distributions. By judgment, the first group of the spike was concerned and the data packet was zoomed again in 500 data intervals. Figure 6 shows the actuating signals for each of the testing. Consistence settings are required to ensure the wavelet generates similar wave perturbation throughout the experiment.

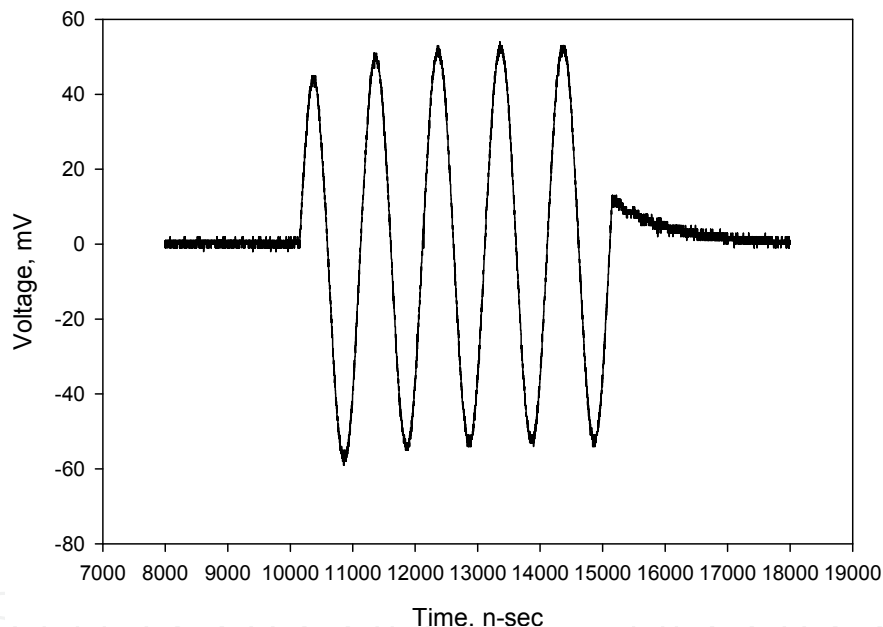


Figure 5. Actuating signals

Figure 7 shows the results of the receiving wave packet upon synthesized by the points for each condition. Different behavior from the voltage (V_{pp}) and complete time of flight cycle are shown which characterized the evaluated conditions.

Then, each of the receiving structural conditions wavelet data were compared between to ensure the signals was homogeneous to each other on the timeline basis. Since this is the unsupervised learning process the clusters were assigned to separate three conditions as stated in the methodology. The V_{pp} or voltage peak to peak is the attribute to distinguish the conditions. More than 50 V_{pp} values were collected and tabulated. The scattering of the V_{pp} for the three conditions were examined and is shown in Figure 8.

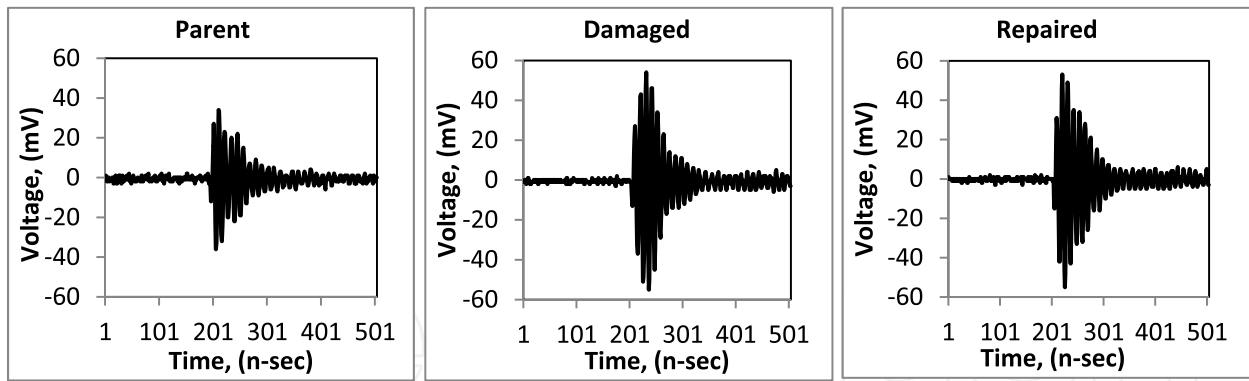


Figure 6. Wave packet samples from a) undamaged, b) damaged and c) repaired structural conditions after synthesized.

The V_{pp} showed similar values for the undamaged and damaged structure condition. It was assumed that the wave travel without discontinuity due to partial damage at that particular area. However several other types of damage need to be examined before any conclusive evidence can be finalized.

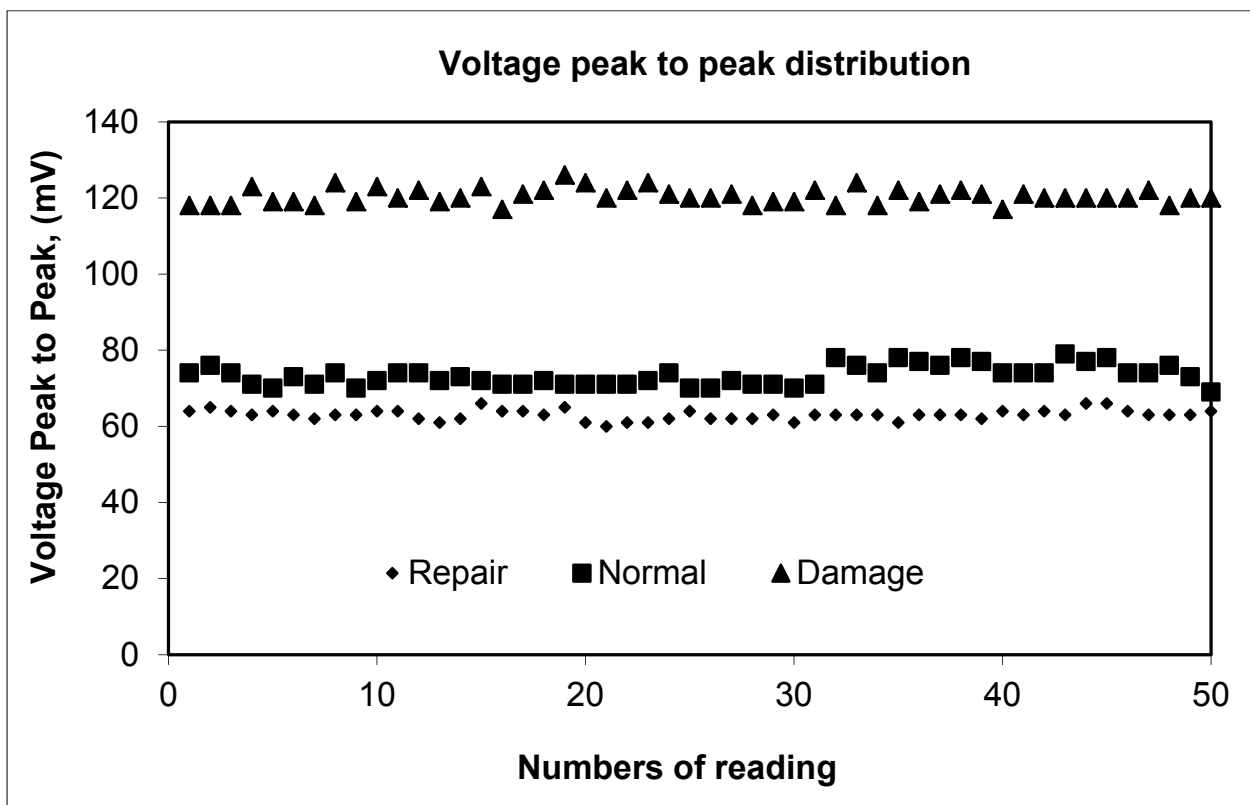


Figure 7. V_{pp} distribution among the structural conditions

A further post processing was carried out by overlapping the three conditions in one graph with similar time-domain comparison. The most common interest point lies within points 12250 ~ 12750. This was the first spike seen in the wave packet. In the earlier V_{pp} comparison, the distribution data between the damage and undamaged were identical. Therefore it was difficult to interpret the data for the latter machine learning process.

However, when all three data was overlapped, a significant different can be seen as shown in Figure 9. The undamaged signals appear at the initial time frame indicated that there was a clean surface wave traveling from the actuator to the receiver. However, once the partial damage was introduced, the spike appear later about 200nsec due to the discontinuity of the spoiler surface. The unaffected wave bifurcated to the receiver with delay. For the repair condition, since the surface integrity has been restored by the flush repair, the continuity of the surface wave was preserved again with delay about 50 nsec .

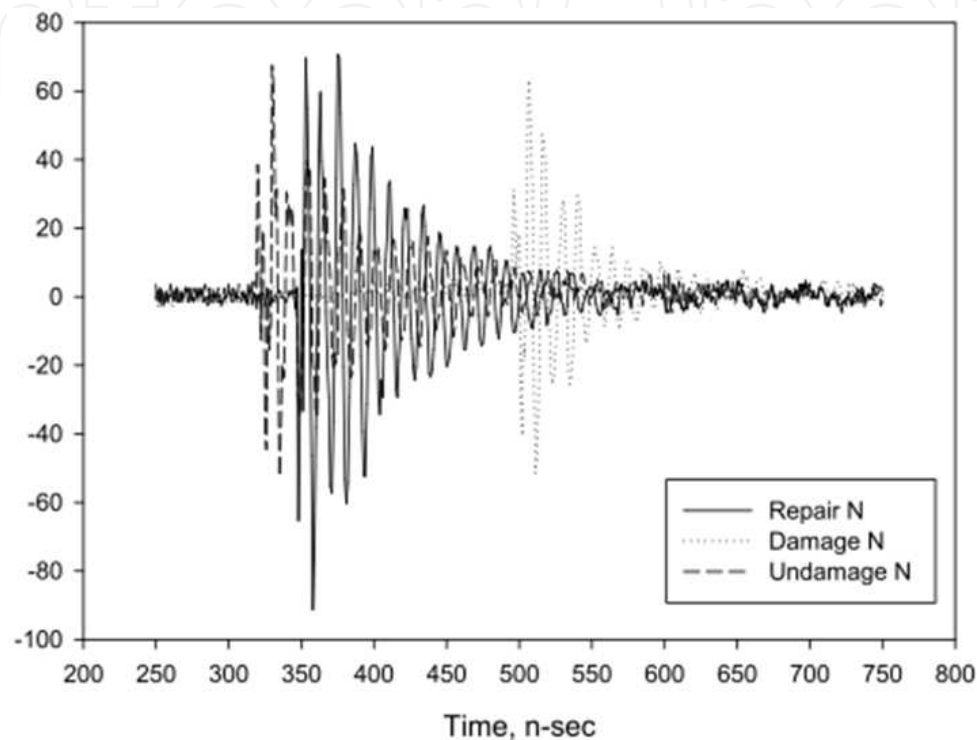


Figure 8. Overlay Outlier Pattern for different structural condition

4.2. Tensile testing

The tensile test results showed a similar behavior towards a brittle stress-strain curve. Below are the results of the tensile test on normal and repaired specimens. All specimens were found to have breakage at center. The fiber breakage for parent specimens occurred at arbitrary layer. However, for the repaired specimens, the breakage occurred at the intermediate bonding layer between the original layers and repair plies. This is due to the fiber discontinuity and the matrix is the only medium to transfer the stress from the parent surface to the repair surface.

Based of the wavelet analysis from the Sigmaplot software, both conditions showed a significant changes at the investigated stages. At the elastic range, the wavelet shows a significant solid wave at the respective time of flight. However a slight change appeared after the first ply failure occurred. The V_{pp} values were found to be higher and there are also a distinct echo developed after the main wave packets. At the end of the testing, the signal lost its signature due to damage upon breakage of the panels. An online monitoring during the course of the test shown a good unique characteristics for anomalies to be identified.

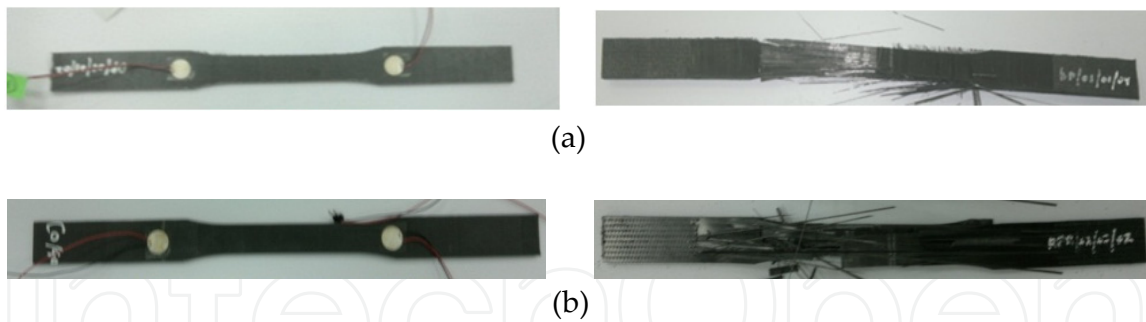


Figure 9. CFRP result before and after tensile test for parent specimens for a) normal and b) repaired specimens

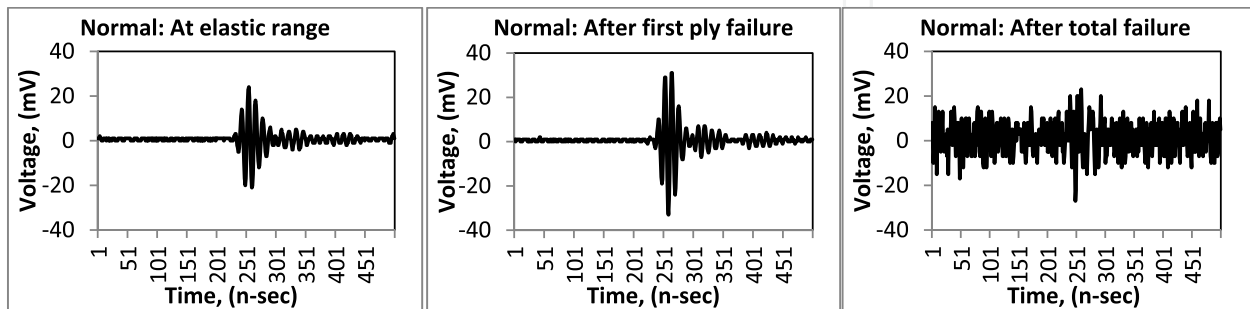


Figure 10. Receiving signals for parent panel with a) at elastic range, b) after first ply failure and c) at failure.

Figure 11 shows the behavior of the full repair panel throughout the testing. The degradation of the signal indicates the lamb wave attenuation has lost due to separation of the repair plies. This can be seen by 50% reduction of the V_{pp} at the initial of the testing. The significant reduction of the signal strength correlates with the structural integrity lost as the test reached the total fractured. Towards the end of the testing, all the specimen failed at the center and disintegration of the sensor due to the failure of the panels.

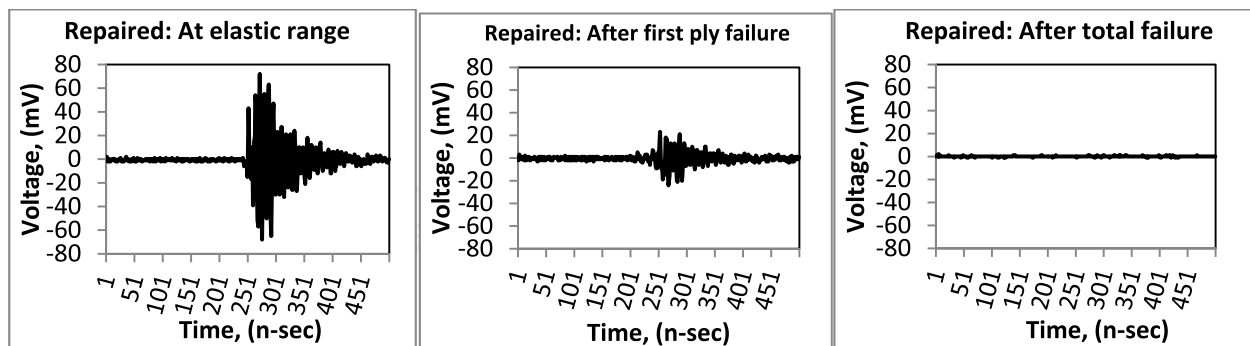


Figure 11. Receiving signals for parent panel with a) at elastic range, b) after first ply failure and c) at failure.

5. Discussion

Both results from the experiments shows a promising indicator on the usage of PZT sensors to monitor structure integrity of the aerospace components and controlled testing specimen. Results from the spoiler shows:-

1. The V_{pp} value for all tested condition showed a significant different due to the signal intensity once it passed the tested conditions. Although the undamaged and damaged signals are almost identical, the repair area shows a higher V_{pp} values. This might due to the additional plies of the repair and the bouncing of the intensification of the signal to travel the tested structure. The time of flight for the repaired reading was found to be delayed from the two conditions. The additional ply or doubler may contribute to the delay. This can promote detection of hidden repair area. The outlier behavior of the V_{pp} is an initial indications that PZT sensors can be used to detect interested conditions.
2. The overlay patten analysis show a promising results as it can bifurcate each of the conditions. The outlier analysis can be applied to differentiate the condition of the surface integrity. Due to separation of the fibers, the time for the Lamb wave to travel from the actuator to the receiver has been delayed and takes a longer time with the reduction of the V_{pp} value when compared to the repaired area.
3. The tensile test indicates that the materials behave in accordance with typical brittle materials. The breakage at the center indicates a good distribution of the load during the testing. The wavelet signals at the elastic area, within the first ply failure and total failure shows good indications of how the Lamb wave behaves before the specimen fails. However, the method of taking the PZT sensor receiver reading need to be improved as the fluctuation of the signals is unbearable.
4. Further post processing techniques need to be used in order to further scrutinize the behavior of the data. A more confident result can be further utilize for more converging result such as by generic algorithm, neural network etc. in order to enhance the prognosis of the structure at later stages.

6. Conclusion

As conclusion, both experiments has proved that PZT sensors can be used to detect anomalies of the CFRP structure either passive or active sensing. In passive sensing, the data received data is very stable and shows a significant consistence reading at any duration. The latter experiment shows that the ability of the sensors to sense structural integrity of a normal and repaired specimens. However, further investigations are required to this robust detection system in order to ensure the results are established. This can be done by comparing the results through various techniques, statistical methods and analytical analysis.

Author details

K.D. Mohd Aris

Universiti Kuala Lumpur, Malaysian Institute of Aviation Technology, Jalan Jenderam Hulu, Selangor, Malaysia

F. Mustapha, S.M. Sapuan, D.L. Majid

Universiti Putra Malaysia, Serdang, Selangor, Malaysia

Acknowledgement

This research is part of Ministry of Science and Technology, Malaysia (MOSTI) SF000064 Escience Fund grant and Spirit Aerosystem (Malaysia) Inc. for donating the aircraft spoiler.

7. References

- [1] The World Wide Composite Industry Structure, Trends and Innovation: New 2010 release, JEC Composite, 2010
- [2] Soutis C. and Diamanti K., Structural Health Monitoring Techniques for Aircraft Composite Structures, *Progress in Aerospace Sciences* 46(2010), 342 -353)
- [3] Baker A., Dutton S. and Kelly D., Joining of Composite Structure, *Composite Materials for Aircraft Structure*, AIAA Inc., 2004. 290 ~295.
- [4] Baker A., Dutton S. and Kelly D., Repair Technology, *Materials for Aircraft Structure*, AIAA Inc., (2004), 290 ~295.
- [5] Mujica L.E. et al., Impact Damage Detection in Aircraft Composites Using Knowledge-Based Reasoning, *Structural Health Monitoring* (2008); 7; 215~230,
- [6] Xie Jian, Lu Yao, Study on Airworthiness Requirements of Composite Aircraft Structure for Transport Category Aircraft in FAA, *Procedia Engineering*, Volume 17 (2011), 270-278
- [7] Kim I. and Park C.Y., Prediction of Impact Forces on an Aircraft Composite Wing, *J. of Intelligent Materials Systems and Structures*, Vol 19, (2008), 319 ~ 324,
- [8] S.M. Sapuan, F. Mustapha, D.L. Majid, Z. Leman, A.H.M. Ariff, M.K.A. Ariffin, M.Y.M. Zuhri, M.R. Ishak and J. Sahari, Fiber Reinforced Composite Structure with Bolted Joint – A Review, *Key Engineering Materials*, 471-472, pg 939-944
- [9] G. Goulios, Z. Marioli-Riga, Composite patch repairs for commercial aircraft: COMPRES, *Air & Space Europe*, Volume 3, Issues 3–4, (2001), 143-147
- [10] S.B. Kumar, S. Sivashanker, Asim Bag, I. Sridhar, Failure of aerospace composite scarf-joints subjected to uniaxial compression, *Materials Science and Engineering: A*, Volume 412, Issues 1–2, (2005), 117-122
- [11] Dan He, Toshiyuki Sawa, Takeshi Iwamoto, Yuya Hirayama, Stress analysis and strength evaluation of scarf adhesive joints subjected to static tensile loadings, *International Journal of Adhesion and Adhesives*, Volume 30, Issue 6, (2010), 387-392
- [12] Chang F. K and Ihn J. B., Pitch Catch Active Sensing Methods in Structural Health Monitoring for Aircraft Structures, *Structural Health Monitoring* (2008) Vol 7, 5~ 19.
- [13] Inman D.J. et al, *Damage Prognosis for Aerospace, civil and Mechanical Systems*, John Wiley and Sons Ltd., 2005
- [14] Ostachowicz W. M., Damage Detection of Structures Using Spectral Finite Element Method, *Computers and Structures* 86 (2008), 454 ~ 462.
- [15] Kesavan A., John S and Herszberg, Structural Health Monitoring of Composite Structures Using Artificial Intelligence Protocol, *Journal of Intelligent Material Systems and Structures*; 19;63, 63 ~ 72

- [16] Worden K, Manson G and Filler N. R. J. , Damage Detection Using Outlier Analysis, *Journal of Sound and Vibration* 229(3) (2000), 647 ~ 667),
- [17] Webb A.R, *Statistical Pattern Recognition*, John Wiley and Sons Ltd, 2002
- [18] F. Mustapha, G. Manson, K. Worden, S.G. Pierce, Damage location in an isotropic plate using a vector of novelty indices, *Mechanical Systems and Signal Processing*, Volume 21, Issue 4, May 2007, Pages 1885-1906
- [19] Charles R Farrar and K. Worden, An introduction to structural health monitoring, *Phil. Trans. R. Soc. A* 15 February 2007 vol. 365 no. 1851 303-315
- [20] Ihn J and Chang F. K., Pitch Catch Active Sensing Methods in Structural Health Monitoring for Aircraft Structures, *Structural Health Monitoring* 2008 Vol. 7, 1 ~ 19.
- [21] Webb A.R, *Statistical Pattern Recognition*, John Wiley and Sons Ltd, 2002) (Park et al, An Outlier Analysis Framework for Impedance Based Structural Health Monitoring System, *Journal of Sound and Vibration* 286 (2005), 229 ~ 250
- [22] *Piezoelectric Ceramics: Principles and Applications*, APC International Ltd, (2008)
- [23] *Boeing 737-300 Structural Repair Manual*, The Boeing Company Inc., 1996
- [24] *Heatcon Composite Systems: Composite Repair Solutions*, Product Catalog, 2011